Supramolecular organization of photosystem I and light-harvesting complex I in *Chlamydomonas reinhardtii*

Marta Germano[a,b,1], Alevtyna E. Yakushevska[c,1], Wilko Keegstra[c], Hans J. van Gorkom[b], Jan P. Dekker[a,*], Egbert J. Boekema[c]

[a] *Faculty of Sciences, Department of Physics and Astronomy, Vrije Universiteit, De Boelelaan 1081, 1081 HV Amsterdam, The Netherlands*
[b] *Biophysics Department, Huygens Laboratory, Leiden University, P.O. Box 9504, 2300 RA Leiden, The Netherlands*
[c] *Department of Biophysical Chemistry, Groningen Biomolecular Sciences and Biotechnology Institute, University of Groningen, Nijenborgh 4, 9747 AG Groningen, The Netherlands*

Received 13 May 2002; revised 8 July 2002; accepted 9 July 2002

First published online 24 July 2002

Edited by Ulf-Ingo Flügge

Abstract **We report a structural characterization by electron microscopy and image analysis of a supramolecular complex consisting of photosystem I and light-harvesting complex I from the unicellular green alga *Chlamydomonas reinhardtii*. The complex is a monomer, has longest dimensions of 21.3 and 18.2 nm in projection, and is significantly larger than the corresponding complex in spinach. Comparison with photosystem I complexes from other organisms suggests that the complex contains about 14 light-harvesting proteins, two or three of which bind at the side of the PSI-H subunit. We suggest that special light-harvesting I proteins play a role in the binding of phosphorylated light-harvesting complex II in state 2.** © **2002 Federation of European Biochemical Societies. Published by Elsevier Science B.V. All rights reserved.**

Key words: Photosystem I; Light-harvesting complex I; Electron microscopy; State transitions; *Chlamydomonas reinhardtii*

1. Introduction

Photosystem I (PSI) is a multi-subunit pigment–protein complex embedded in the thylakoid membranes of green plants and cyanobacteria. It consists of two functionally and structurally different domains: the core complex and the peripheral antenna. The core complex contains all electron transport cofactors required to oxidize plastocyanin or cytochrome *c* and to reduce ferredoxin or flavodoxin. It consists of two large membrane-intrinsic subunits, called PsaA and PsaB, and, depending on the species, 10–12 small intrinsic or extrinsic proteins located at the periphery of the two large subunits [1,2]. The structure of the core complex of the cyanobacterium *Synechococcus elongatus* has been resolved at 2.5 Å resolution [3–5]. Under most physiological conditions, the PSI core complex occurs as a trimer in cyanobacteria and as a monomer in eukaryotic organisms (green plants).

The peripheral antenna of PSI is fundamentally different in various groups of organisms. In cyanobacteria, membrane-extrinsic phycobilisomes act as peripheral antenna systems for both photosystem II (PSII) and PSI under normal growth conditions, though under iron limitation a membrane-intrinsic chlorophyll (Chl) *a* binding protein called IsiA or CP43′ replaces phycobilisomes in the peripheral antenna function. Recent electron microscopy (EM) studies revealed that 18 copies of the IsiA protein form a closed ring around the trimeric PSI core complex of *Synechocystis* PCC 6803 [6] and *Synechococcus* PCC 7942 [7]. Oceanic *Prochlorococcus* species were also shown to have a ring of 18 membrane-intrinsic Chl *a/b* binding Pcb antenna proteins around the trimeric PSI core complex [8]. Green plants contain a peripheral antenna complex known as light-harvesting complex I (LHCI), composed of four distinct polypeptides (Lhca1–4) belonging to the group of Chl *a/b* binding proteins of the Lhc super-gene family [9]. In higher plants, approximately two copies of each of these polypeptides bind to the (monomeric) PSI core complex. EM studies have indicated that all LHCI bind at the side of the PSI-F and PSI-J subunits of the PSI core complex [10], the same side at which the peripheral IsiA and Pcb antenna proteins bind in cyanobacteria and *Prochlorococcus* [6–8]. Furthermore, when plants are illuminated with light that preferentially excites PSII (the so-called state 2 conditions [11,12]), a part of LHCII is phosphorylated and may also bind to the PSI core complex, probably at the PSI-H subunit [13].

In this report, we investigate the supramolecular organization of the PSI–LHCI complex of the unicellular green alga *Chlamydomonas reinhardtii* by EM and image analysis. This alga is widely used as an experimental organism and model system for the study of the biogenesis of the photosynthetic apparatus, the mechanisms by which the photosynthetic apparatus respond to changing environmental conditions, and for the genetic analysis of chloroplast function [14]. The peripheral antenna of *C. reinhardtii* also consists of Chl *a/b* binding proteins of the Lhc super-gene family, but it may be composed of as many as 10 different polypeptides [15]. Our results indicate that the LHCI antenna of *C. reinhardtii* consists of about 14 LHCI proteins, two or three of which cover the PSI-H site of the PSI core complex. It is possible that the latter LHCI proteins play a crucial role in the state transitions in this organism.

*Corresponding author. Fax: (31)-20-4447999.
E-mail address: dekker@nat.vu.nl (J.P. Dekker).

[1] These two authors contributed equally to this work.

Abbreviations: β-DM, *n*-dodecyl-β-D-maltoside; Chl, chlorophyll; EM, electron microscopy; LHCI, light-harvesting complex I; MSA, multivariate statistical analysis; PSI, photosystem I; PSII, photosystem II

PII: S0014-5793(02)03100-9

2. Materials and methods

C. reinhardtii strain CC-2137 wild-type cells were grown mixotrophically in Tris–acetate–phosphate medium [16] and harvested during the late exponential phase of growth (at a Chl concentration of 20 μg/ml). Cells were suspended in buffer A (20 mM HEPES–HCl, pH 7.5, 2 mM $MgCl_2$, 0.35 M sorbitol and 10 mM EDTA) and disrupted by sonication (power 60 W in 10 cycles of 10 s with 20 s waiting time). Thylakoid membranes were partially purified by differential centrifugation, and finally resuspended in buffer B (25 mM Bis–Tris, pH 6.0, 10 mM NaCl, 5 mM $CaCl_2$).

Thylakoids were incubated in buffer B with 1.25% (w/v) *n*-dodecyl-β-D-maltoside (β-DM) at a concentration of 1.33 mg Chl/ml for 30 min at room temperature. Subsequent centrifugation at 40 000 × *g* to remove unsolubilized material revealed that more than 90% of the total Chl was extracted by this detergent treatment. The supernatant was overlaid on sucrose gradients (prepared by freezing and thawing centrifuge tubes containing 32 ml of a 25% (w/v) sucrose solution in buffer B+0.03% (w/v) β-DM) and the gradients were centrifuged at 150 000 × *g* (70Ti, Beckmann) for about 20 h. All steps (except for the thylakoid detergent extraction) were performed at 4°C. The concentration of Chl was determined according to Arnon [17]. SDS–PAGE was performed as in [18] and pigment analysis was performed according to [19].

EM specimens were prepared on glow-discharged carbon-coated grids, using 2% uranyl acetate as negative stain. Electron microscopy was performed on a Philips CM10 electron microscope at 52 000× magnification. Images were scanned with a Nikon Coolscan 8000 ED at 20 μm, equivalent to 3.85 Å at the specimen level. From 65 digitized negatives 17 822 projections were selected for single particle averaging [20] with Groningen Image Processing (GRIP) software. Projections were aligned by, in GRIP-implemented, multi-reference alignment using mutual correlation functions [21]. The aligned images were subjected to multivariate statistical analysis (MSA). The MSA program was highly parallelized, which gave a reduction in computing time of about 80% (on eight computers). The core routines used and the parallel version of the householder-QL matrix diagonalization algorithm were obtained from J.S. Reeve [22]. After MSA, particles were classified and summed and class sums were used in a next cycle of multi-reference alignment, MSA and classification.

3. Results

The separation of β-DM-solubilized thylakoid membranes of *C. reinhardtii* by sucrose density gradient centrifugation resulted in three main green bands. On the basis of SDS–PAGE (Fig. 1A) and the absorption spectrum (Fig. 1B), the lowest band was identified as PSI–LHCI complexes and corresponded to 25–30% of the total Chl in the thylakoid extract, while the middle and upper bands contained PSII core complexes and LHCII, respectively. SDS–PAGE analysis of the lowest band (Fig. 1A, second lane) reveals a polypeptide composition very similar to that reported by Bassi et al. [15] and Pineau et al. [23] for *C. reinhardtii* PSI–LHCI complexes. There are at least five different types of major polypeptides between 20 and 27 kDa and also some minor bands, in agreement with the suggestion of Bassi et al. [15] that at least 10 different polypeptides contribute to the peripheral antenna of *C. reinhardtii*. The major bands of LHCII (Fig. 1A, first lane) were strongly reduced in the fraction with the PSI–LHCI complexes. The content of LHCII resembles the LHCII content of stroma lamellae purified from state 1-adapted maize plants and is much smaller than the LHCII content observed in stroma lamellae from state 2-adapted maize plants [24], from which we conclude that the *C. reinhardtii* particles of our study represent PSI in state 1. A comparison of the absorption spectra of PSI–LHCI from *C. reinhardtii* and PSI-200 from *Arabidopsis thaliana* (Fig. 1B) shows that the Chl *a*/*b* ratio is smaller in *C. reinhardtii*, as well as the content of 'red pigments' (between 700 and 725 nm). HPLC analysis (not shown) revealed a Chl *a*/*b* ratio of 4.5 and low levels (two molecules per 100 Chl *a*) of neoxanthin and loroxanthin, the major carotenoids of LHCII in *C. reinhardtii* [23], in agreement with the results in [23] and with the strong reduction of LHCII proteins in our PSI–LHCI complexes (see above).

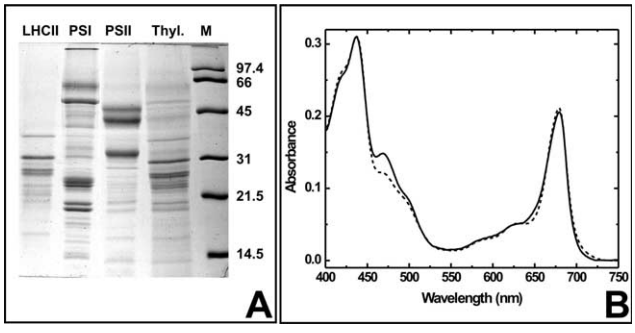

Fig. 1. A: SDS–PAGE analysis of the three green bands from the sucrose gradients. Lane 1 (upper green band), Lhcb polypeptides (including LHCII); lane 2 (lowest green band), PSI-LHCI complex; lane 3 (intermediate green band), PSII core complex; lane 4, thylakoid membranes; lane 5, markers (their molecular weights, in kDa, are indicated on the right). B: Room temperature absorption spectra of PSI–LHCI complexes from *C. reinhardtii* (solid line) and *Arabidopsis thaliana* (dashed line). The spectra were normalized at 436 nm.

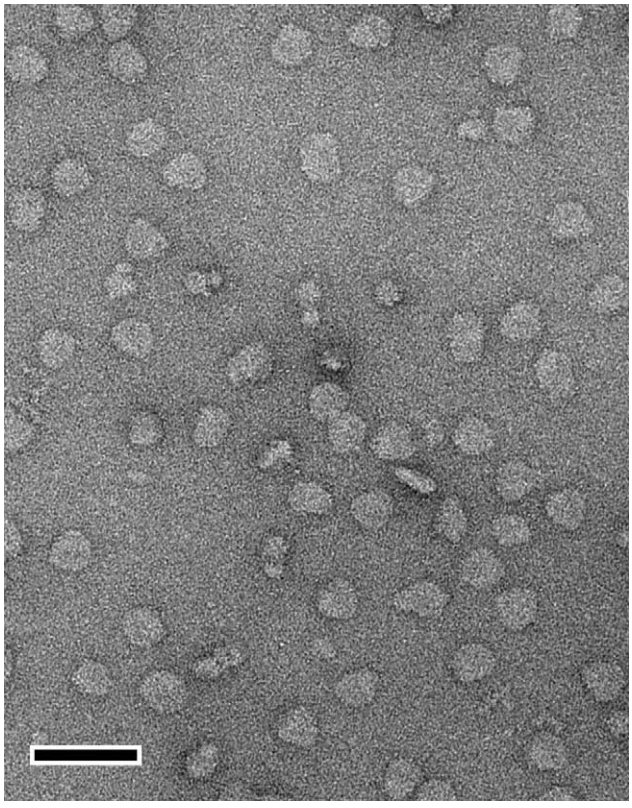

Fig. 2. Part of an electron micrograph showing mainly top view projections of PSI complexes, negatively stained with 2% uranyl acetate. The scale bar is 50 nm.

EM images of the PSI–LHCI complexes indicate a monomeric aggregation state. Oval-shaped top view projections of uniform size dominate the sample (Fig. 2), but a few proton

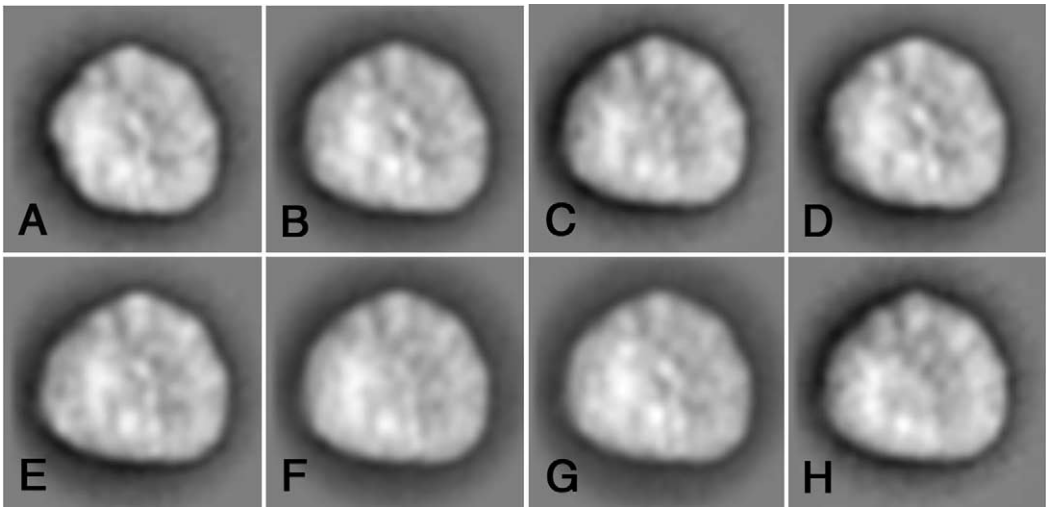

Fig. 3. Single particle analysis of top view projections of *C. reinhardtii* PSI–LHCI complexes. A–H: The eight best classes (out of 10), found by classification of 17 822 projections. Each class sum consists of 1500 top view projections on average.

ATPase complexes were also present. A large set of top view projections was processed by single particle analysis. After several cycles of alignment of projections, comparison by multivariate statistical analysis and subsequent classification, the set of 17 822 images was divided into 10 classes, eight of which are shown in Fig. 3. The class sums indicate surprisingly little variation in the overall shape of the particle, indicating a rather homogeneous subunit composition. Only in two classes (Fig. 3A,D) a significant reduction of mass is observed, indicating the loss of one or more subunits at the left side of the complex. Except for two classes (not shown) fine detail in the interior part of the projections was well preserved and the final resolution in the best classes was 1.4 nm, as determined by Fourier ring correlation [25].

The final sum of the best 1037 projections of the *C. reinhardtii* PSI–LHCI complex shows dimensions of 21.3 nm × 18.2 nm, with a surface area of 299 nm^2 in projection (Fig. 4A). It is substantially larger than the PSI-200 complex from spinach (Fig. 4B, 227 nm^2 in projection), and almost as large as the trimeric PSI core complex from cyanobacteria (Fig. 4C, 332 nm^2 in projection). The summed projection of the class in Fig. 3A has a surface area of 259 nm^2 in projection.

4. Discussion

The position of the monomeric PSI core complex within the PSI–LHCI particles shown in Fig. 4A can be deduced from a comparison of density profiles. This position should coincide with the most stain-excluding areas of the projection map, caused by the presence of several extrinsic proteins bound to the core complex. Fig. 4D–F shows how the surfaces of the cyanobacterial PSI core (red overlay) and the PSI-200 complex from spinach (yellow overlay) fit within the *C. reinhardtii* PSI–LHCI complex. The black asterisks in Fig. 4D–F indicate a pronounced density profile, which presumably arises from the PsaF and PsaJ subunits of the PSI core complex. The high-resolution model from X-ray diffraction can be fitted into this position as shown in Fig. 4G.

Attempts to fit the PSI core complex in orientations significantly different from the one shown in Fig. 4D did not result in a satisfactory superposition of the density profiles. In addition, relative positions of LHCI and the PSI core much different from the one proposed here would not be compatible with the existing information on subunit–subunit interactions in *C. reinhardtii* PSI. In particular, a rotation of the PSI core by 180° would place the PSI-F subunit near the lower left corner of the complex, away from the LHCI domain. Such an orientation would be in disagreement with the proposed close connection between PSI-F and the LHCI antenna in *C. reinhardtii* [26].

Most of the peripheral antenna subunits must be at the upper right side of the complex (Fig. 4D), the same side as in the plant PSI–LHCI complex. The results of the classification of the *C. reinhardtii* PSI–LHCI projections (Fig. 3) suggest a remarkably uniform size and shape of this part of the complex. In the PSI-200 complexes from spinach, substantial numbers of particles with a partially reduced peripheral antenna were found by classification [10].

A comparison between the LHCI areas in *C. reinhardtii* and spinach shows that the additional proteins in *C. reinhardtii* are found at two positions at the lower left and upper right sides of the complex. The additional proteins at the upper right side are organized in a concentric zone around inner LHCI subunits (Fig. 4D). The additional lower left part of the PSI–LHCI structure is absent or reduced in a minority of the projections (Fig. 3A,D), in which the contours at the left side resemble those of the spinach PSI-200 projections [10], the side at which presumably the PSI-H and PSI-L subunits are located. The missing mass in Fig. 3A has an area of about 40 nm^2, consistent with that of about three monomeric LHC-type proteins (the area of an LHCII monomer is 12 nm^2 [27]). The elongated shape of the missing mass in Fig. 3A is, however, too narrow to be occupied by a trimeric LHCII complex.

These results imply that the known differences between *C. reinhardtii* and higher plants in the extent of the state transitions [12] could originate from the structure of the PSI–LHCI complexes. In *Arabidopsis*, state transitions do not occur without the PSI-H protein [13], which can be explained by the binding, in state 2, of phosphorylated LHCII to the PSI-H protein of the PSI–LHCI complex [11]. In our PSI–LHCI complexes from *C. reinhardtii*, however, the PSI-H subunit

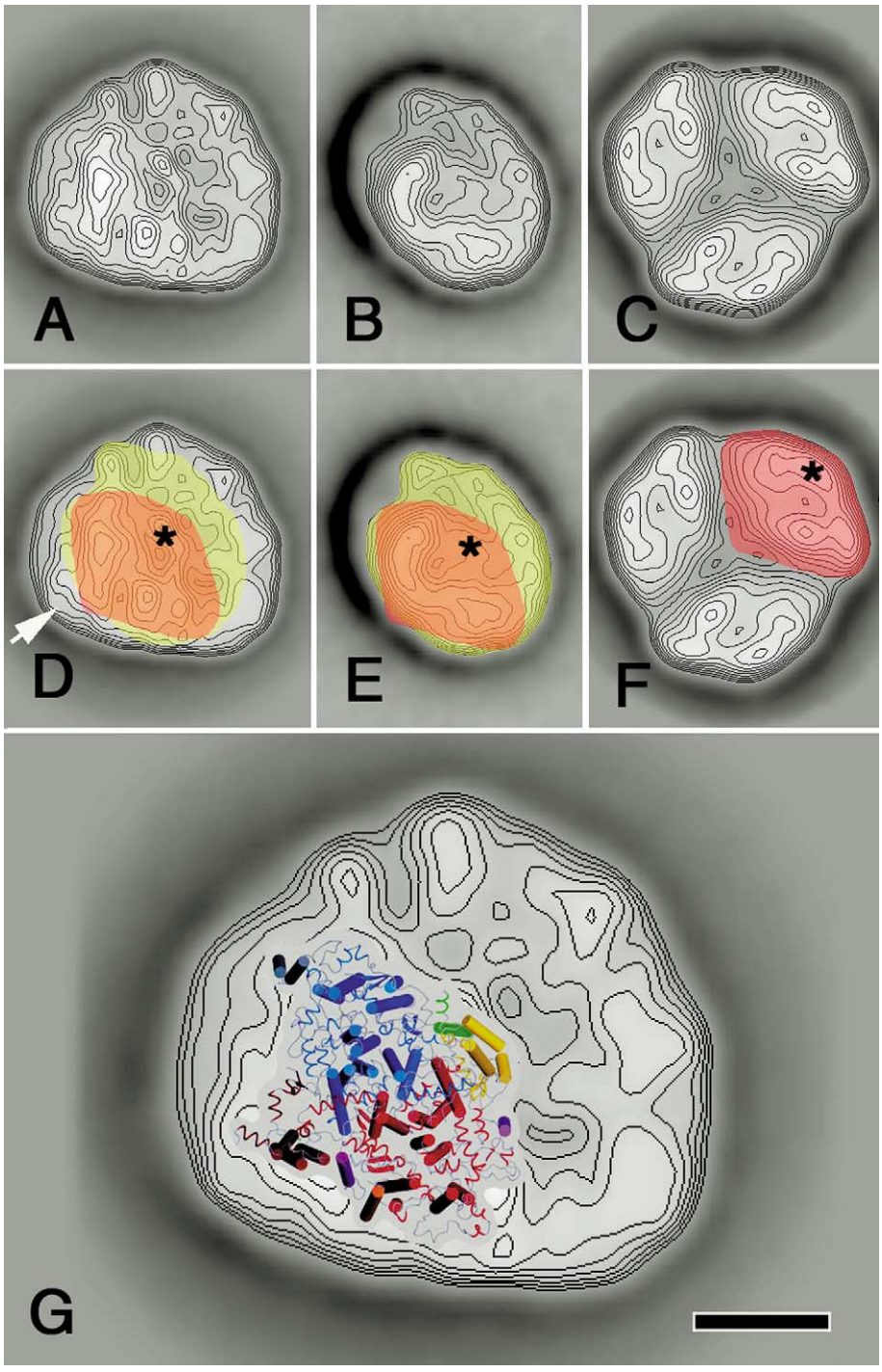

Fig. 4. Comparison of the PSI–LHCI complexes from *C. reinhardtii* (A,D,G, the best 1037 projections from classes B, and E to H of Fig. 3), spinach (B,E, from [10]) and a trimeric PSI core complex from a cyanobacterium (C,F, from [31]). D–F: The projections of A–C, but with a red overlay to indicate the position of the (cyanobacterial) PSI core complex (D–F) and a yellow overlay to indicate the position of the PSI-200 complex from spinach (D,E). The white arrow marks a site which is present in most PSI–LHCI monomers from *C. reinhardtii*, but absent in monomers from spinach. G: The *C. reinhardtii* PSI–LHCI projection with a high-resolution X-ray model of the PSI core complex from *Synechococcus elongatus* superimposed (from [4]). The yellow and green α-helices in G belong to the PsaF and PsaJ subunits. The black asterisks in D–F indicate the density which coincides with the position of the PsaF/PsaJ subunits. The complexes are viewed from the stromal side onto the membrane plane. The assignment of the position of the PSI core complex in the projection in B is also based on projections of better-resolved dimeric aggregates of PSI-200 [10]. Scale bar in G is 5 nm.

seems to be exposed only in a minor part of the complexes (the classes shown in Fig. 3A,D), while in the other classes one or more proteins with a mass similar to that of two or three monomeric LHC types of protein seem to cover the PSI-H part of the core complex. With the presently available information, we cannot exclude that an LHCII type of complex is responsible for (part of) the additional mass at this position, in view of the results from SDS–PAGE (Fig. 1) and pigment analysis. It is, however, also possible that special LHCI protein(s) at the left side of the *C. reinhardtii* PSI–LHCI complex

function to facilitate the binding of one or more phosphorylated LHCII complexes.

For an estimation of the number of LHCI subunits in the *C. reinhardtii* PSI–LHCI complexes, it is necessary to estimate the contribution of detergent to the area of the projections. A reliable estimation for this detergent contribution is possible for cyanobacterial PSI trimers. Averaged sums of negatively stained trimers, prepared, imaged and processed in a similar way as performed for *C. reinhardtii* PSI–LHCI complexes (Fig. 4C), have a maximal radius of 11.2 nm. The X-ray space-filling model indicates a maximal radius of 10.5 nm [3], so the detergent contribution is about 0.7 nm. With a detergent layer of 0.7 nm, the surface area of the *C. reinhardtii* PSI–LHCI complex converts to 261 nm^2. Because the surface of 1/3 cyanobacterial PSI trimer is close to 90 nm^2 [28], the peripheral antenna would have an area of 170 nm^2 (assuming that the PSI core complexes in plants and cyanobacteria occupy the same area). If this space were covered by LHCI monomers with a surface area of 12 nm^2 each [27], about 14 copies of monomeric LHCI proteins would be present. This number is not far from the earlier estimate of 12 LHCI proteins per complex [29]. A similar calculation of the area of the PSI-200 complex from spinach [10] leads to a detergent-corrected value of 190 nm^2 for PSI-200, or 100 nm^2 for the LHCI part, in agreement with the presence of eight monomeric LHCI proteins. We conclude that the size of the peripheral LHCI antenna is almost twice as large in *C. reinhardtii* as in spinach. A recent proteomics approach revealed 18 different LHCI proteins, though at least some of these are thought to be the result of post-translational modifications and some occurred in very low quantities [30].

Acknowledgements: We thank Ineke de Boer and Dré de Wit for the expert growing of the *C. reinhardtii* cells and Henny van Roon for performing pigment analysis. M.G. acknowledges Grant PRAXISX-XI/BD/2870/94 from the Portuguese National Foundation for Scientific and Technical Research (JNICT). This research was supported by the Netherlands Foundation for Scientific Research (NWO) via the Foundation for Life and Earth Sciences (ALW).

References

[1] Chitnis, P.R. (2001) Annu. Rev. Plant Physiol. Plant Mol. Biol. 52, 593–626.
[2] Scheller, H.V., Jensen, P.E., Haldrup, A., Lunde, C. and Knoetzel, J. (2001) Biochim. Biophys. Acta 1507, 41–60.
[3] Jordan, P., Fromme, P., Witt, H.T., Klukas, O., Saenger, W. and Krauss, N. (2001) Nature 411, 909–917.
[4] Fromme, P., Jordan, P. and Krauss, N. (2001) Biochim. Biophys. Acta 1507, 5–31.
[5] Saenger, W., Jordan, P. and Krauss, N. (2002) Curr. Opin. Struct. Biol. 12, 244–254.
[6] Bibby, T.S., Nield, J. and Barber, J. (2001) Nature 412, 743–745.
[7] Boekema, E.J., Hifney, A., Yakushevska, A.E., Piotrowski, M., Keegstra, W., Berry, S., Michel, K.-P., Pistorius, E.K. and Kruip, J. (2001) Nature 412, 745–748.
[8] Bibby, T.S., Nield, J., Partensky, F. and Barber, J. (2001) Nature 413, 590.
[9] Jansson, S. (1999) Trends Plant Sci. 4, 236–240.
[10] Boekema, E.J., Jensen, P.E., Schlodder, E., van Breemen, J.F.L., van Roon, H., Scheller, H.V. and Dekker, J.P. (2001) Biochemistry 40, 1029–1036.
[11] Haldrup, A., Jensen, P.E., Lunde, C. and Scheller, H.V. (2001) Trends Plant Sci. 6, 301–305.
[12] Wollman, F.-A. (2001) EMBO J. 20, 3623–3630.
[13] Lunde, C., Jensen, P.E., Haldrup, A., Knoetzel, J. and Scheller, H.V. (2000) Nature 408, 613–615.
[14] Hippler, M., Redding, K. and Rochaix, J.-D. (1998) Biochim. Biophys. Acta 1367, 1–62.
[15] Bassi, R., Soen, S.Y., Frank, G., Zuber, H. and Rochaix, J.-D. (1992) J. Biol. Chem. 267, 25714–25721.
[16] Gorman, D.S. and Levine, R.P. (1965) Proc. Natl. Acad. Sci. USA 54, 1665–1669.
[17] Arnon, D.I. (1949) Plant Physiol. 42, 1–15.
[18] Laemmli, U.K. (1970) Nature 227, 680–685.
[19] Peterman, E.J.G., Gradinaru, C.C., Calkoen, F., Borst, J.C., van Grondelle, R. and van Amerongen, H. (1997) Biochemistry 36, 12208–12215.
[20] Harauz, G., Boekema, E. and van Heel, M. (1988) Methods Enzymol. 164, 35–49.
[21] Van Heel, M., Schatz, M. and Orlova, E. (1992) Ultramicroscopy 46, 307–316.
[22] Reeve, J.S. and Heath, M. (1999) Parallel Comput. 25, 311–319.
[23] Pineau, B., Gérard-Hirne, C. and Selve, C. (2001) Plant Physiol. Biochem. 39, 73–85.
[24] Vallon, O., Bulte, L., Dainese, P., Olive, J., Bassi, R. and Wollman, F.-A. (1991) Proc. Natl. Acad. Sci. USA 88, 8262–8266.
[25] Van Heel, M. (1987) Ultramicroscopy 21, 95–100.
[26] Hippler, M., Biehler, K., Krieger-Liszkay, A., van Dillewijn, J. and Rochaix, J.-D. (2000) J. Biol. Chem. 275, 5852–5859.
[27] Kühlbrandt, W., Wang, D.N. and Fujiyoshi, Y. (1994) Nature 367, 614–621.
[28] Schubert, W.-D., Klukas, O., Krauss, N., Saenger, W., Fromme, P. and Witt, H.T. (1997) J. Mol. Biol. 272, 741–769.
[29] De Vitry, C., Wollman, F.-A. and Delepelaire, P. (1983) CR Acad. Sci. Sect. III 297, 277–280.
[30] Hippler, M., Klein, J., Fink, A., Allinger, T. and Hoerth, P. (2001) Plant J. 28, 595–606.
[31] Mangels, D., Kruip, J., Berry, S., Rögner, M., Boekema, E.J. and Koenig, F. (2002) Photosynth. Res., in press.